Size control of magnetite nanoparticles by organic solvent-free chemical coprecipitation at room temperature

Tomohiro Iwasaki[a]; Naoya Mizutani[a]; Satoru Watano[a]; Takeshi Yanagida[b]; Tomoji Kawai[b]
[a] Department of Chemical Engineering, Osaka Prefecture University, Osaka, Japan [b] Institute of Scientific and Industrial Research, Osaka University, Osaka, Japan

PLEASE SCROLL DOWN FOR ARTICLE

Taylor & Francis
Taylor & Francis Group

Size control of magnetite nanoparticles by organic solvent-free chemical coprecipitation at room temperature

Tomohiro Iwasaki[a]*, Naoya Mizutani[a], Satoru Watano[a], Takeshi Yanagida[b] and Tomoji Kawai[b]

[a]*Department of Chemical Engineering, Osaka Prefecture University, Osaka, Japan;* [b]*Institute of Scientific and Industrial Research, Osaka University, Osaka, Japan*

This study provides a facile single-step coprecipitation method for preparing size-controlled high crystalline magnetite nanoparticles in water system without using any organic solvents. In this method, an iron ions solution and an alkaline solution are simply mixed at room temperature without using any additional heating treatment. The size of obtained magnetite nanoparticles greatly depended on the coexisting anionic species in the starting solution because the coexisting anions greatly influenced both the formation of crystal nuclei and the dispersion stabilisation of formed precipitates. The size control of magnetite nanoparticles having high crystallinity and ferromagnetic property could be successfully achieved by using the effects of coexisting anions. For synthesising finer magnetite nanoparticles, the presence of lactate ion in the starting solution was effective, and coarser ones could be synthesised under higher ferrous/ferric ions molar ratios.

Keywords: Fe_3O_4; magnetic nanoparticle; coprecipitation; anion; iron complex

1. Introduction

Magnetite (Fe_3O_4) is one of the most useful industrial materials because of its excellent magnetic properties, and Fe_3O_4 nanoparticles have been used in various industrial products, such as recording media, pigments, copying toners, etc. The efficiency of such industrial products greatly depends on the size of Fe_3O_4 nanoparticles. Thus, the particle size has been controlled to be suitable for their applications by means of various preparation techniques using chemical reactions under dry and wet conditions. In biomedical applications, particularly, precise control of the particle size is required. For example, for drug delivery system Lin et al. [1] and Zhang and Misra [2] synthesised the Fe_3O_4 nanoparticles of about 20 nm and 5 nm using a liquid phase coprecipitation method and a thermal decomposition method, respectively. Wang et al. [3] applied the Fe_3O_4 nanoparticles of about 20 nm synthesised by an electrochemical deposition method for cancer therapy.

Many preparation methods of Fe_3O_4 nanoparticles developed so far have several significant problems. In many cases, the synthesis process is complicated and

*Corresponding author. Email: iwasaki@chemeng.osakafu-u.ac.jp

environment-unfriendly organic solvents are often used, resulting in an increase in both production costs and environmental impact. However, coprecipitation techniques in water systems without using any organic solvents are promising as a useful preparation method because the synthesis process can be simplified and the environmental impact is relatively low. In widely used coprecipitation methods, hydroxides of ferrous and ferric ions, ferrous hydroxide ($Fe(OH)_2$) and goethite (α-FeOOH), are coprecipitated as precursors in an alkaline solution at relatively low temperature. The molar ratio of ferrous ion to ferric ion is 0.5, corresponding to the chemical stoichiometric ratio of Fe_3O_4 formation reaction [4]. Then the solid phase reaction between the hydroxides results in the formation of Fe_3O_4. Recent reports reveal that the size of Fe_3O_4 nanoparticles thus formed greatly depends on the concentration of ferrous and ferric ions [5] and the reaction temperature [6]. These results imply that the synthesis conditions influence greatly not only the Fe_3O_4 formation reaction but also the formation of $Fe(OH)_2$ and α-FeOOH precipitates. Accordingly, in order to control the size of Fe_3O_4 nanoparticles, the formation process of $Fe(OH)_2$ and α-FeOOH precipitates should be also controlled. Kandori et al. [7,8] reported that the formation and crystal growth of α-FeOOH colloids was influenced by the anionic species existing together with ferric ions in the solution. Therefore, the coexisting anions must play an important role in the formation of Fe_3O_4 nanoparticles, and the function of coexisting anions should be clarified for controlling the particle size. To our knowledge, however, there is no research focusing on the effect of coexisting anions in the synthesis of Fe_3O_4 nanoparticles using the coprecipitation method.

Coprecipitation methods for preparing Fe_3O_4 nanoparticles also have a serious problem. The formed Fe_3O_4 nanoparticles tend to have relatively low crystallinity, leading to poor magnetic property, when the coprecipitation is carried out at low temperature. Thus, a heating process, such as annealing and hydrothermal treatment is often employed to improve the crystallinity [6,9]. Unfortunately, this complicates the synthesis process and spoils the advantages of this method. In addition, it is very difficult to prepare ultrafine Fe_3O_4 nanoparticles with a size of 10 nm or less because the $Fe(OH)_2$ and α-FeOOH precipitates and the Fe_3O_4 nanoparticles tend to aggregate owing to heating even though their size before heating is less than 10 nm [6]. This reduces controllable range of the particle size. Accordingly, the heating process is unsuitable for the size control of Fe_3O_4 nanoparticles [10].

In this study, for preparing size-controlled high crystalline Fe_3O_4 nanoparticles without any heating treatment, a facile single-step coprecipitation process using effects of coexisting anions has been developed. In this method, an iron ions solution and an alkaline solution are simply mixed at room temperature. It is expected that the effects can contribute not only to control the particle size but also to improve the crystallinity because the reaction rate of Fe_3O_4 formation may vary depending on the coexisting anionic species. Influence of the kind and amount of coexisting anions on the size and crystallinity of obtained Fe_3O_4 nanoparticles was examined. The role of coexisting anions in the formation process of Fe_3O_4 nanoparticles is discussed.

2. Experimental

2.1. *Synthesis of Fe₃O₄ nanoparticles*

All chemicals used in the experiments were of analytical reagent grade and were used without further purification. In all the experiments, ferric chloride hexahydrate

($FeCl_3 \cdot 6H_2O$) was used as the ferric ion source. As the ferrous ion source, ferrous sulphate heptahydrate ($FeSO_4 \cdot 7H_2O$) and ferrous chloride tetrahydrate ($FeCl_2 \cdot 4H_2O$), which are often used in many studies on the synthesis of Fe_3O_4 nanoparticles, were used. In addition, ferrous lactate trihydrate ($Fe(C_3H_5O_3)_2 \cdot 3H_2O$) was also used because ferric ion has a tendency to form a relatively stable complex with lactate ion $C_3H_5O_3^-$ unlike sulphate ion SO_4^{2-} and chloride ion Cl^- [11]. $FeCl_3 \cdot 6H_2O$ of 2 mmol and 1 mmol of one of the above-mentioned ferrous ion salts were dissolved in 40 mL of deionised and deoxygenated water. Sodium hydroxide (NaOH) solution of 20 mL of 1.0 kmol/m^3 was dropped into the solution at room temperature under vigorous stirring using a magnetic stirrer. The addition rate of NaOH solution was kept at constant of 3.0 mL/min for forming the precipitates homogeneously. When the NaOH solution was added to the iron salts solution, $Fe(OH)_2$ and α-FeOOH were coprecipitated and then Fe_3O_4 was formed by the solid phase reaction between them, according to the following chemical reactions.

$$Fe^{2+} + 2OH^- \rightarrow Fe(OH)_2$$
$$Fe^{3+} + 3OH^- \rightarrow Fe(OH)_3$$
$$Fe(OH)_3 \rightarrow \alpha\text{-FeOOH} + H_2O$$
$$Fe(OH)_2 + 2\alpha\text{-FeOOH} \rightarrow Fe_3O_4 + 2H_2O.$$
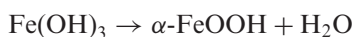
After addition of the NaOH solution, the pH value of the suspension was higher than 12. These operations were carried out under argon atmosphere to prevent the oxidation of ferrous ion. The resulting precipitate was immediately washed with deionised water and decanted after centrifugation at centrifugal acceleration of 1500 G. The washing operation was repeated thrice, and then the sample was dried at 30°C under vacuum for 5 h.

In order to investigate the role of anion (SO_4^{2-}, Cl^- and $C_3H_5O_3^-$) during the formation of Fe_3O_4 nanoparticles, 1 mmol of sodium sulphate (Na_2SO_4), 2 mmol of sodium chloride (NaCl) or 2 mmol of sodium lactate ($NaC_3H_5O_3$) was added to the water before the iron salts were dissolved. Furthermore, for increasing the reaction rate, the molar ratio of ferrous ions to ferric ions was increased as 1.0 and 2.0 in the $FeSO_4$–$FeCl_3$ system without adding any additives [12]. The experimental conditions are summarised in Table 1.

Table 1. Experimental conditions.

Run #	Ferrous ions source	Additive	Ferrous/ferric ions molar ratio
1	$FeSO_4$	–	0.5
2	$FeCl_2$	–	0.5
3	$Fe(C_3H_5O_3)_2$	–	0.5
4	$FeSO_4$	NaCl	0.5
5	$FeSO_4$	$NaC_3H_5O_3$	0.5
6	$FeCl_2$	Na_2SO_4	0.5
7	$FeCl_2$	$NaC_3H_5O_3$	0.5
8	$FeSO_4$	–	1.0
9	$FeSO_4$	–	2.0

2.2. *Characterisation*

The morphology of prepared samples was observed with a field emission scanning electron microscope (FE-SEM; JSM-6700F, JEOL). The hydrodynamic size distribution (number basis) was measured by dynamic light scattering (DLS; DLS-7000, Otsuka Electronics) and the median diameter was determined. The powder X-ray diffraction (XRD) pattern was measured with Cu-Kα radiation ranging from $2\theta = 10°$ to $80°$ at a scanning rate of $1.0°$/min using a Rigaku RINT-1500 powder X-ray diffractometer. The average crystallite size was calculated from the full-width at half-maximum (FWHM) of the Fe_3O_4 (311) diffraction peak at $2\theta \approx 35.5°$ using Scherrer's formula. The lattice constant was also determined from several diffraction angles showing high intensity peak. The magnetic property (magnetisation–magnetic field hysteretic cycle) was analysed using a super-conducting quantum interference device (SQUID) magnetometer (model MPMS, Quantum Design) at room temperature in the rage of magnetic field between -10 and $10\,kOe$. In order to investigate the dispersion stability of precipitates in water containing the anions, the zeta potential of Fe_3O_4 nanoparticles (synthesised under the conditions of Run #2) in the solution containing a proper amount of Na_2SO_4, NaCl or $NaC_3H_5O_3$ was evaluated with a zeta potential analyser (Zetasizer Nano ZS, Malvern Instruments). Furthermore, for evaluating the relative stability of ferric complex with the anions, the UV analysis [13] for the $0.2\,mM$ $FeCl_3$ solutions containing $0.2\,mM$ of either Na_2SO_4 or $NaC_3H_5O_3$ was carried out at room temperature using a spectrophotometer (Ubest V-530, JASCO).
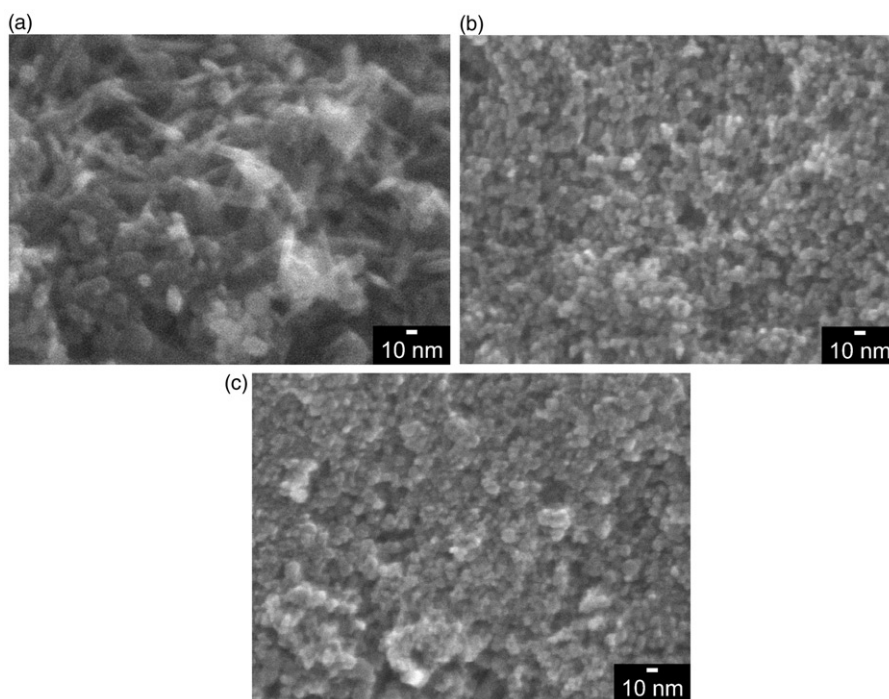

Figure 1. SEM images of the samples of Run #1 (a), #2 (b) and #3 (c).

3. Results and discussion

Figures 1 and 2 show, respectively, SEM images and XRD patterns of the samples obtained under the conditions of Run #1–#3. As can be seen in Figures 1(a) and 2(a), when $FeSO_4$ was used as the ferrous ion source, the formation reaction of Fe_3O_4 was uncompleted and unreacted α-FeOOH (acicular-shaped particles) were contained in the sample, since the reaction is slow at room temperature. When either $FeCl_2$ or $Fe(C_3H_5O_3)_2$ was used instead of $FeSO_4$, however, the reaction rate increased relatively and the single phase of Fe_3O_4 formed. Figures 3 and 4 show, respectively, SEM images and XRD patterns of the samples of Run #4–#7. In the cases of addition of NaCl (Run #4) and $NaC_3H_5O_3$ (Run #5) in the $FeSO_4$–$FeCl_3$ system, similar results to Run #2 and #3 were obtained, respectively. This reveals that Cl^- and $C_3H_5O_3^-$ can promote the solid phase reaction between α-FeOOH and $Fe(OH)_2$ even though $FeSO_4$ is used, resulting in rapid formation of single Fe_3O_4 phase. The size of Fe_3O_4 nanoparticles prepared in the presence of SO_4^{2-} (i.e. in Run #4–#6) was relatively large compared with the cases without SO_4^{2-} (Runs #2 and #3). Thus, SO_4^{2-} was found to have the effect to increase the particle size. On the other hand, Cl^- and $C_3H_5O_3^-$ effectively contributed to size reduction of the Fe_3O_4
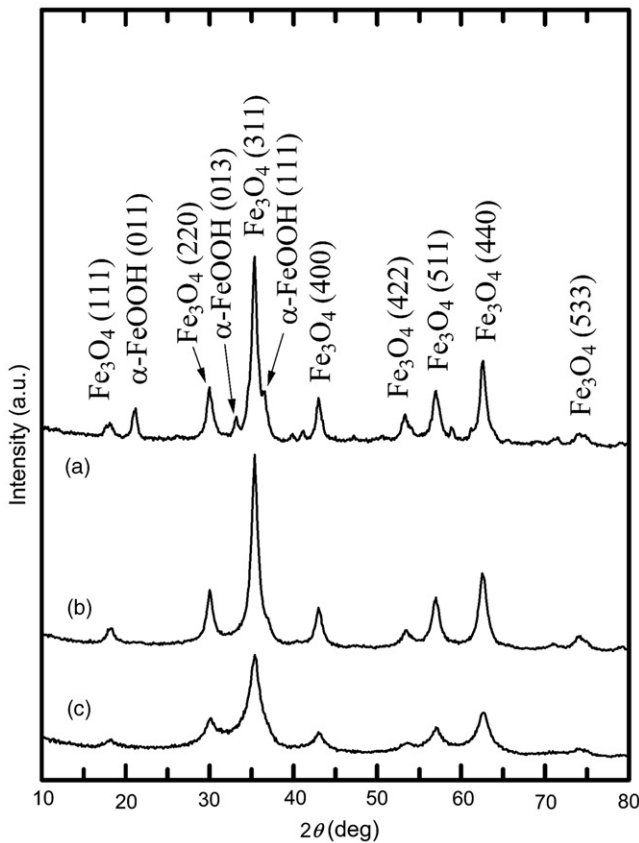

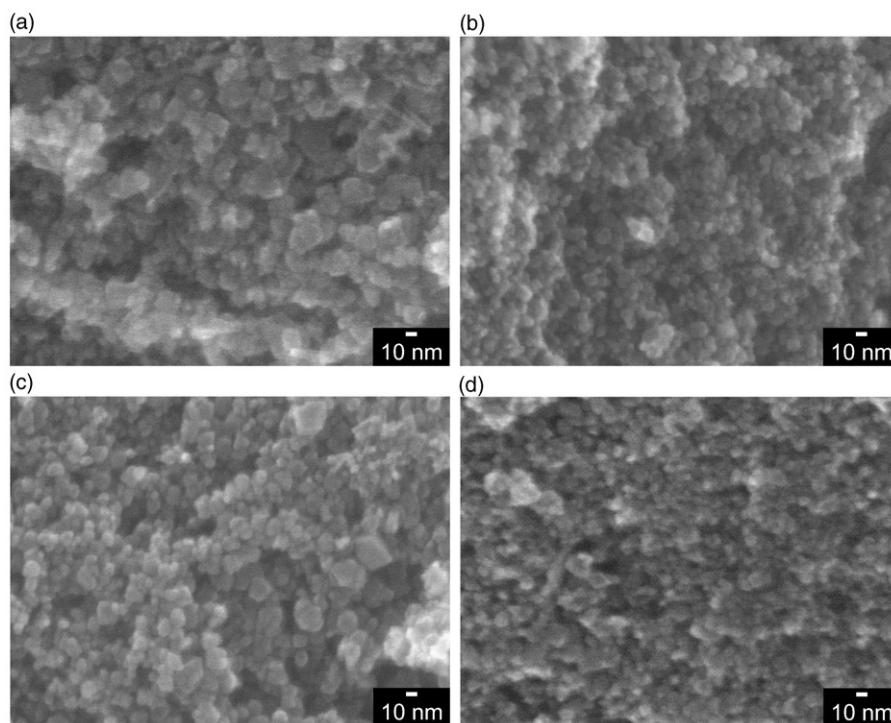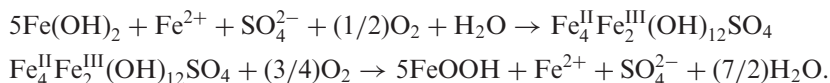Figure 2. XRD patterns of the samples of Run #1 (a), #2 (b) and #3 (c).

Figure 3. SEM images of the samples of Run #4 (a), #5 (b), #6 (c) and #7 (d).

nanoparticles, as shown in Figures 1(b), (c) and 3(d). The results suggest that the coexisting anionic species can be the operational factor to control the particle size.

Subsequently, in order to prepare coarser Fe_3O_4 nanoparticles, the amount of $FeSO_4$ in the starting solution was increased without adding any additives. Figures 5 and 6 show, respectively, SEM images and XRD patterns of the samples obtained under the conditions of Runs #8 and #9. When the ferrous/ferric ions molar ratio was higher than the stoichiometric ratio (=0.5), the reaction rate increased and the single Fe_3O_4 phase formed. The particle size increased with increasing molar ratio because of the effect of SO_4^{2-}. At higher ferrous/ferric ions molar ratios, $Fe(OH)_2$ remains in the suspension containing SO_4^{2-}. In this case, a small amount of oxygen contained in the solution oxidises a part of $Fe(OH)_2$ at room temperature, resulting in the formation of α-FeOOH via a green rust $(Fe_4^{II}Fe_2^{III}(OH)_{12}SO_4)$ [14,15] according to the following reactions [16].

$$5Fe(OH)_2 + Fe^{2+} + SO_4^{2-} + (1/2)O_2 + H_2O \rightarrow Fe_4^{II}Fe_2^{III}(OH)_{12}SO_4$$

$$Fe_4^{II}Fe_2^{III}(OH)_{12}SO_4 + (3/4)O_2 \rightarrow 5FeOOH + Fe^{2+} + SO_4^{2-} + (7/2)H_2O.$$

The green rust functioned as a buffer and promoted the coprecipitation of $Fe(OH)_2$ and α-FeOOH, leading to the growth of Fe_3O_4 nanoparticles.

Table 2 gives properties of the samples of Run #2–#9. The median size almost agreed with the average crystallite size. This means that the obtained Fe_3O_4 nanoparticles had a
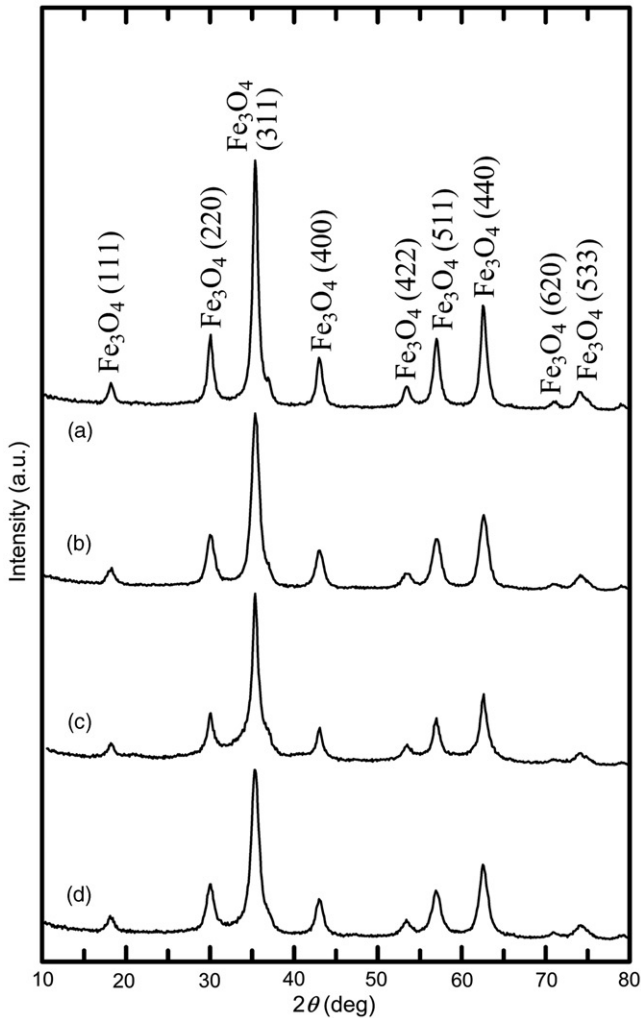
Figure 4. XRD patterns of the samples of Run #4 (a), #5 (b), #6 (c) and #7 (d).

single-crystal structure, i.e. high crystallinity. In XRD patterns of the samples of Run #2–#9 shown in Figures 2, 4 and 6, the diffraction intensity peaks indicating formation of other compounds were not observed. In addition, the lattice constant was between 8.386 and 8.404 Å and close to the standard value of Fe_3O_4 ($=8.396$ Å) compared with that of maghemite ($=8.345$ Å). These results also suggest that the samples had a single Fe_3O_4 phase regardless of the experimental conditions. The samples of Run #2–#9 exhibited a ferromagnetic behaviour with a relatively high saturation magnetisation. However, the value decreased with the particle size and was lower than that of the corresponding bulk (about 90 emu/g) due to their smaller size [17]. The coercivity also decreased with the particle size, and the samples with a size of less than approximately 10 nm had very low coercivity, indicating superparamagnetism.
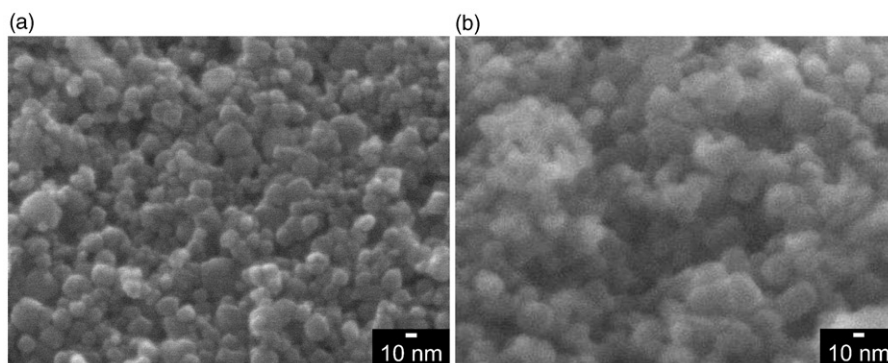
Figure 5. SEM images of the samples of Run #8 (a) and #9 (b).

It is well known that ferrous and ferric ions in iron salts solutions form iron hydroxo-complex ions and/or ferrosic complex ions and in alkaline solutions iron hydroxides with different crystalline structures, depending on environmental conditions precipitate [18–20]. If anions in the solution directly take part in the formation reaction of iron hydroxides as reactive species, part of hydroxide ions OH^- in the iron hydroxides may be replaced by the anions, resulting in formation of specific iron hydroxides depending on the anionic species. This leads to formation of iron oxides with completely different properties. However, many studies demonstrated that uniform Fe_3O_4 was obtained from the iron salts solutions containing SO_4^{2-} and/or Cl^-. Inoue and Hatta [21] also reported that no anions in the solution replaced OH^- in the formed ferric hydroxides although the crystalline structure depended strongly on the anionic species. In our experimental results, single Fe_3O_4 phase was obtained regardless of combination of the anionic species as mentioned earlier. Consequently, it is considered that lactate ion $C_3H_5O_3^-$ also does not directly take part in the formation reaction of Fe_3O_4. This means that the formation process proceeds according to the same chemical reaction regardless of the anionic species.

From the results of Run #2–#5, the size of Fe_3O_4 nanoparticles obtained in the presence of $C_3H_5O_3^-$ was smaller than those in the presence of Cl^-. When SO_4^{2-} coexisted in the solution, the effect of $C_3H_5O_3^-$ was reduced. Furthermore, when $FeCl_2$ was used as the ferrous ion source, the Fe_3O_4 nanoparticles obtained in the presence of SO_4^{2-} (Run #6) and $C_3H_5O_3^-$ (Run #7) became coarser and finer, respectively, as compared with that without adding any additives (Run #2). The result of Run #4 almost agreed with that of Run #6. In addition, the experiments under several combinations of ferrous ion sources and sodium salts excluding those shown in Table 1 were carried out. For example, when $Fe(C_3H_5O_3)_2$ was used and either Na_2SO_4 or $NaCl$ was added, the obtained results (data not shown) were almost the same as those of Run #5 and #7, respectively. The results reveal that the particle size greatly depends on the coexisting anionic species regardless of its source. Consequently, it was confirmed that the size of Fe_3O_4 nanoparticles could be controlled by a combination of the coexisting anions.

The values of zeta potential of Fe_3O_4 nanoparticles in the Na_2SO_4, $NaCl$ and $NaC_3H_5O_3$ solutions were –19.2, –21.8 and –31.2 mV, respectively. $C_3H_5O_3^-$ was found to be effective to decrease the surface potential of Fe_3O_4 nanoparticles. As can be seen in
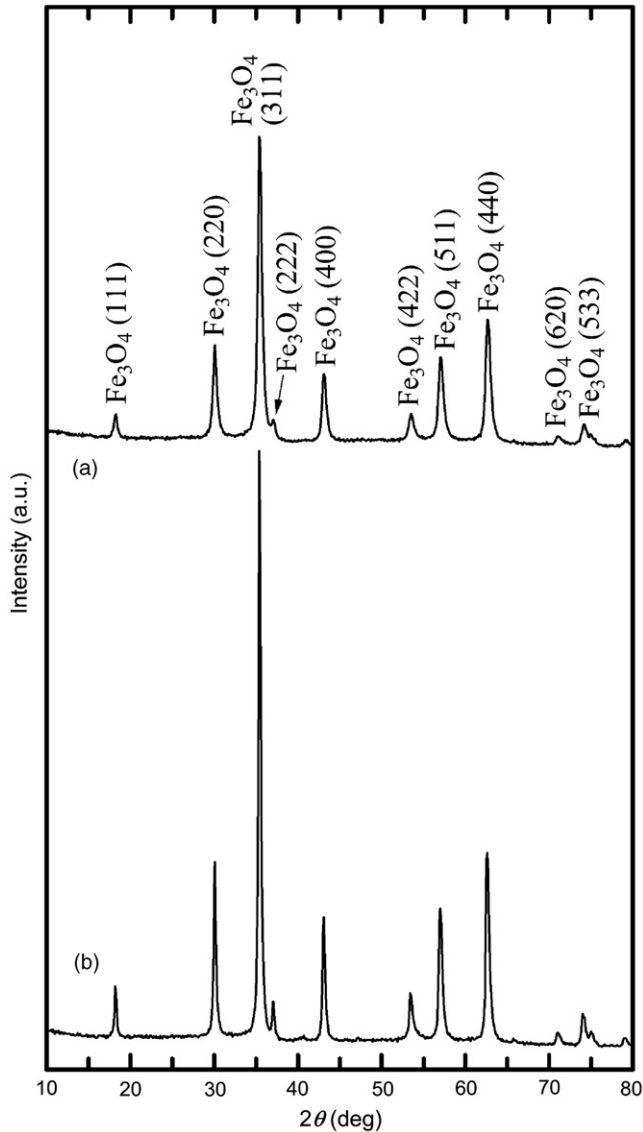
Figure 6. XRD patterns of the samples of Run #8 (a) and #9.

Table 2, when anions reducing the zeta potential coexisted in the starting solution, the obtained Fe_3O_4 nanoparticles had a tendency to become finer. Therefore, it was clarified that the decrease in the surface potential by anions, i.e. the increase in the dispersion stability of Fe_3O_4 nanoparticles, contributed effectively to the decrease in the particle size. This suggests that the effect may also be shown for the iron hydroxides precipitates. Figure 7 shows the UV spectra of ferric ion solutions containing SO_4^{2-}, Cl^- and $C_3H_5O_3^-$. UV spectrum of the ferric ion solution containing both SO_4^{2-} and Cl^- had a strong

Table 2. Properties of samples.

Run #	Median size (nm)	Average crystallite size (nm)	Lattice constant ($\mathring{A}$)	Saturation magnetisation (emu/g)	Coercivity (Oe)
2	9.9	10.9	8.402	47.1	3
3	4.9	4.9	8.386	59.4	6
4	15.2	11.4	8.397	56.5	4
5	11.5	7.6	8.390	56.3	3
6	15.0	9.7	8.390	51.8	3
7	6.6	7.4	8.404	62.2	5
8	16.8	14.8	8.388	63.4	12
9	24.6	25.3	8.392	67.9	65
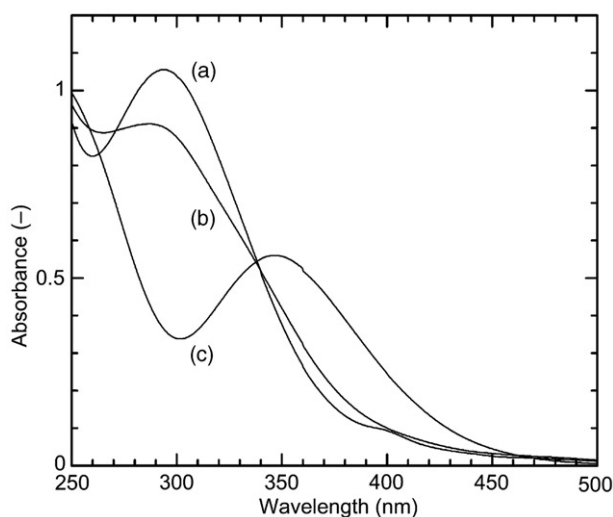
Figure 7. UV spectra of the solutions of (a) $FeCl_3$, (b) $FeCl_3 + Na_2SO_4$ and (c) $FeCl_3 + NaC_3H_5O_3$.

absorption peak at a wavelength of approximately 290 nm, which was similar to that of the $FeCl_3$ solution without adding any sodium salts. When $C_3H_5O_3^-$ coexisted with Cl^-, however, the UV spectrum greatly changed and the strong absorption peak was observed at a wavelength of 347 nm. It was confirmed that formation of the ferric complex with Cl^- is hardly influenced by SO_4^{2-} and that $C_3H_5O_3^-$ forms the complex more easily with ferric ion than Cl^-. This result implies that among these anions $C_3H_5O_3^-$ forms the most stable ferric complex and ferric complex with SO_4^{2-} has the lowest stability. Accordingly, the formation mechanism of Fe_3O_4 nanoparticles in this system containing $C_3H_5O_3^-$ may be as follows. In an alkaline solution, ferric ions tend to form relatively stable complex with $C_3H_5O_3^-$ and OH^-, leading to a decrease in the ionic strength of the solution. This promotes the formation of ferric hydroxides, and then the formation of crystal nuclei occurs frequently comparing with the particle growth, resulting in the formation

of finer precipitates. Furthermore, the surface potential of formed Fe_3O_4 nanoparticles decreases by adsorption of $C_3H_5O_3^-$ onto their surface. This results in promotion of the dispersion stabilisation in the suspension, leading to inhibition of the particle growth caused by aggregation. When SO_4^{2-} coexists, the precipitates tend to aggregate each other due to decreasing dispersion stability, resulting in the particle growth. In the presence of Cl^-, the intermediate phenomenon is observed.

4. Conclusions

A facile single-step coprecipitation method has been developed in order to prepare size-controlled high crystalline Fe_3O_4 nanoparticles in water system at room temperature. In the coprecipitation process, the particle size varied greatly depending on the stability of iron complex with the coexisting anions in the starting solution and on the surface potential of anions-adsorbed precipitates, which controlled both the reaction rate of formation of the precipitates and the particle growth. It was concluded that the effects of coexisting anions on the formation of finer Fe_3O_4 nanoparticles increased in the order, $C_3H_5O_3^-$, Cl^-, SO_4^{2-}, corresponding to the stability of iron complex and the surface potential. Therefore, it was confirmed that the size control of Fe_3O_4 nanoparticles could be easily carried out by this method and that the proper selection of coexisting anions according to a desired size was essential. For example, in the synthesis of finer Fe_3O_4 nanoparticles, the use of $Fe(C_3H_5O_3)_2$ as the ferrous iron source was effective; on the other hand, coarser ones could be synthesised under higher ferrous/ferric ions molar ratios. The particle size can be controlled more precisely by adjusting both combination and concentration of the coexisting anions.

References

[1] B.L. Lin, X.D. Shen, and S. Cui, *Application of nanosized Fe₃O₄ in anticancer drug carriers with target-orientation and sustained-release properties*, Biomed. Mater. 2 (2007), pp. 132–134.

[2] J. Zhang and R.D.K. Misra, *Magnetic drug-targeting carrier encapsulated with thermosensitive smart polymer: Core-shell nanoparticle carrier and drug release response*, Acta Biomater. 3 (2007), pp. 838–850.

[3] X. Wang, R. Zhang, C. Wu, Y. Dai, M. Song, S. Gutmann, F. Gao, G. Lv, J. Li, X. Li, Z. Guan, D. Fu, and B. Chen, *The application of Fe₃O₄ nanoparticles in cancer research: A new strategy to inhibit drug resistance*, J. Biomed. Mater. Res. A 80 (2007), pp. 852–860.

[4] S. Lian, E. Wang, Z. Kang, Y. Bai, L. Gao, M. Jiang, C. Hu, and L. Xu, *Synthesis of magnetite nanorods and porous hematite nanorods*, Solid State Commun. 129 (2004), pp. 485–490.

[5] I. Martínez-Mera, M.E. Espinosa-Pesqueira, R. Pérez-Hernández, and J. Arenas-Alatorre, *Synthesis of magnetite (Fe₃O₄) nanoparticles without surfactants at room temperature*, Mater. Lett. 61 (2007), pp. 4447–4451.

[6] J.H. Wu, S.P. Ko, H.L. Liu, S. Kim, J.S. Ju, and Y.K. Kim, *Sub 5 nm magnetite nanoparticles: Synthesis, microstructure, and magnetic properties*, Mater. Lett. 61 (2007), pp. 3124–3129.

[7] K. Kandori, M. Fukuoka, and T. Ishikawa, *Effects of citrate ions on the formation of ferric oxide hydroxide particles*, J. Mater. Sci. 26 (1991), pp. 3313–3319.

[8] K. Kandori, S. Uchida, S. Kataoka, and T. Ishikawa, *Effects of silicate and phosphate ions on the formation of ferric oxide hydroxide particles*, J. Mater. Sci. 27 (1992), pp. 719–728.

[9] J.H. Wu, S.P. Ko, H.L. Liu, M.H. Jung, J.H. Lee, J.S. Ju, and Y.K. Kim, *Sub 5 nm Fe₃O₄ nanocrystals via coprecipitation method*, Colloids Surf. A 313–314 (2008), pp. 268–272.

[10] T. Iwasaki, K. Kosaka, N. Mizutani, S. Watano, T. Yanagida, H. Tanaka, and T. Kawai, *Mechanochemical preparation of magnetite nanoparticles by coprecipitation*, Mater. Lett. 62 (2008), pp. 4155–4157.

[11] M.A. Ali, F. Yasui, S. Matsugo, and T. Konishi, *The lactate-dependent enhancement of hydroxyl radical generation by the Fenton reaction*, Free Radical Res. 32 (2000), pp. 429–438.

[12] N. Mizutani, T. Iwasaki, S. Watano, T. Yanagida, H. Tanaka, and T. Kawai, *Effect of ferrous/ ferric ions molar ratio on reaction mechanism for hydrothermal synthesis of magnetite nanoparticles*, Bull. Mater. Sci. 31 (2008), pp. 713–717.

[13] T. Sugimoto and Y. Wang, *Mechanism of the shape and structure control of monodispersed α-Fe₂O₃ particles by sulfate ions*, J. Colloid Interf. Sci. 207 (1998), pp. 137–149.

[14] J.-M.R. Génin, G. Bourrié, F. Trolard, M. Abdelmoula, A. Jaffrezic, P. Refait, V. Maitre, B. Humbert, and A. Herbillon, *Thermodynamic equilibria in aqueous suspensions of synthetic and natural Fe(II)-Fe(III) green rusts: Occurrences of the mineral in hydromorphic soils*, Environ. Sci. Technol. 32 (1998), pp. 1058–1068.

[15] Ph. Refait, J.-B. Memet, C. Bon, R. Sabot, and J.-M.R. Génin, *Formation of the Fe(II)-Fe(III) hydroxysulphate green rust during marine corrosion of steel*, Corros. Sci. 45 (2003), pp. 833–845.

[16] T. Kuroki, A. Matsumoto, K. Nakatsuka, and N. Tsuchiya, *Influences of Ni²⁺, Co²⁺, Cu²⁺ and Pd²⁺ ions on hydrothermal synthesis of magnetite*, J. Min. Mater. Proc. Inst. Jpn. 119 (2003), pp. 484–488.

[17] J. Lee, T. Isobe, and M. Senna, *Magnetic properties of ultrafine magnetite particles and their slurries prepared via in-situ precipitation*, Colloids Surf. A 109 (1996), pp. 121–127.

[18] J.-P. Jolivet, *Metal Oxide Chemistry and Synthesis: From Solution to Solid State*, John Wiley & Sons, Chichester, 2000.

[19] R.M. Cornell and U. Schwertmann, *The Iron Oxides: Structure, Properties, Reactions, Occurrences and Uses*, Wiley-VCH, Weinheim, 2003.

[20] M. Kiyama, *Conditions for the formation of Fe₃O₄ by the air oxidation of Fe(OH)₂ suspension*, Bull. Chem. Soc. Jpn. 47 (1974), pp. 1646–1650.

[21] A. Inoue and T. Hatta, *Co-precipitation synthesis of Schwertmannite and its analogues with different anion species, focusing on understanding of the role of anions in the formation of FeOOH minerals*, J. Clay Sci. Soc. Jpn. 45 (2006), pp. 250–265.